

Pressure-tuned spin switching in compensated GdCrO₃ ferrimagnet

I. Fita ,* R. Puzniak , and A. Wisniewski *Institute of Physics, Polish Academy of Sciences, Aleja Lotnikow 32/46, PL-02668 Warsaw, Poland*

(Received 17 December 2020; revised 31 January 2021; accepted 4 February 2021; published 16 February 2021)

The effect of hydrostatic pressure on antiferromagnetic ordering of Cr spins, magnetic compensation, and exotic spin switching in the single-crystal GdCrO₃ ferrimagnet is studied. The Néel temperature $T_N = 168$ K increases under pressure with the rate of 0.42 K/kbar, and the compensation temperature $T_{\text{comp}} = 144$ K at which the canted ferromagnetic moment of Cr spins and antiparallel polarized moment of Gd spins cancel each other also increases by 0.3 K/kbar. It was found that the spin switching temperature T_{sw} , at which the ferromagnetic moment is reversed, noticeably increases under pressure, and the spin switching energy required for magnetization reversal reduces significantly because of a decrease in magnetic anisotropy. Due to this mechanism, the spin switching line, described in the T - H diagram by a certain ratio of switching energy to canted ferromagnetic moment, is shifted under pressure towards higher temperatures. Thus, switching between two opposite spin configurations in the GdCrO₃ ferrimagnet can be controlled by both applied magnetic field and external pressure.

DOI: [10.1103/PhysRevB.103.054423](https://doi.org/10.1103/PhysRevB.103.054423)

I. INTRODUCTION

Orthochromite GdCrO₃ exhibits remarkable properties attractive for practical applications, such as ferroelectricity, magnetoelectric effect, and giant magnetocaloric effect [1–5]. Moreover, GdCrO₃ is a compensated ferrimagnet and reveals an exotic phenomenon of negative magnetization, as well as fast spin switching accompanied by magnetization reversal [2,6–9]. Spin switching occurs in this crystal with a large change in magnetic moment over a wide temperature range of ~ 100 K, which provides an ideal scenario for switching devices and, on the other hand, this behavior is interesting for fundamental research. A simple phenomenological model, which assumes a presence of oppositely polarized paramagnetic Gd³⁺ spins with respect to ferromagnetic (FM) moment of canted Cr³⁺ spins, can explain unusual magnetism in GdCrO₃. Weak FM moment along the c axis follows from the canted antiferromagnetic (AFM) ordering of Cr spins at $T_N = 168$ K, caused by the antisymmetric Dzyaloshinskii-Moriya (DM) exchange interaction, while opposite paramagnetic moment of the spin Gd³⁺ is due to strong AFM exchange interaction between Gd³⁺ and Cr³⁺ spins [6,7]. Two opposite moments cancel each other at the compensation temperature $T_{\text{comp}} = 144$ K and below T_{comp} the net FM moment is directed oppositely to weak applied magnetic field, demonstrating a metastable magnetic state with negative magnetization. Spontaneous spin switching to the equilibrium state with positive magnetization and minimum energy occurs when a change in the Zeeman energy upon switching overcomes the anisotropy energy barrier. Similar compensated spin structures and switching between them have been identified in various orthorhombic perovskites RMO_3 ($R =$ rare-earth elements, $M =$ Fe, Cr, Mn) [10–17]. It is interesting to note

that in Er, Nd, and Sm orthoferrites, the spin switching is exchange biased in the vicinity of the compensation temperature, above and below T_{comp} [17], whereas in GdCrO₃ crystal the exchange bias was found above T_{comp} only and is absent below T_{comp} .

Pressure is an effective tool for tuning physical properties of perovskite oxides, and the response of complex crystal structures to high pressure is currently being actively studied [18–20]. It was found that CrO₆ octahedral-site rotations and t - e orbital hybridization play a decisive role in pressure-induced changes in the exchange interactions between Cr spins and in the Néel temperature T_N of $RCrO_3$ orthochromites [18,21]. Moreover, an increase in T_N with a simultaneous decrease in canted FM moment was predicted for SmCrO₃, based on first principles calculations [20]. It was also found that external pressure effect on both magnetic quantities is opposite to the effect of “chemical” pressure, which increases with decreasing R ion size in $RCrO_3$ series [20]. The balance of two opposite magnetic moments in compensated GdCrO₃ can be changed under pressure, if the canted FM moment decreases, as predicted for orthochromites. This stimulated the research of unusual magnetism of GdCrO₃ under high pressure. Here, we show that applied pressure does indeed change the magnetic compensation in GdCrO₃, mainly by decreasing canted FM moment. More interestingly, we found that spin switching temperature T_{sw} markedly increases under pressure due to a strong decrease in magnetic anisotropy. The fact that switching between two opposite spin configurations can be controlled by external pressure well elucidates the nature of magnetic compensation and spin switching in GdCrO₃.

II. EXPERIMENTAL DETAILS

Magnetic study under pressure was carried out on single crystals of GdCrO₃, magnetic properties of which at ambient pressure P have recently been studied in detail [8], in the

*Corresponding author: ifita@ifpan.edu.pl

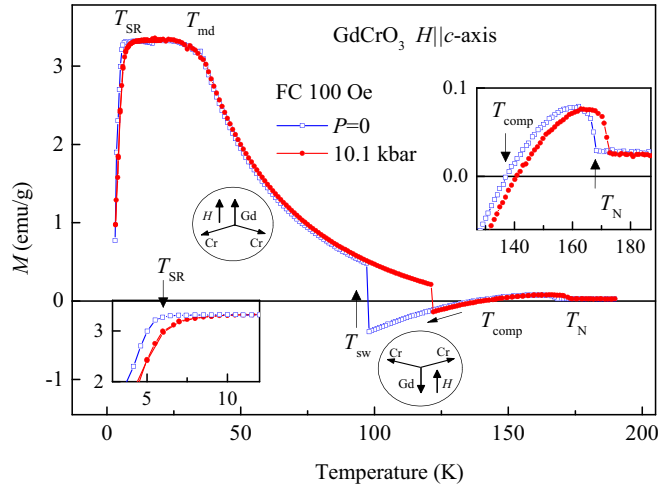


FIG. 1. Temperature dependence of the field-cooled (FC) magnetization of GdCrO_3 single crystal measured in magnetic field applied along the c axis upon cooling in 100 Oe at ambient pressure and at 10.1 kbar. The spin switching temperature T_{sw} , at which the FM moment is reversed, noticeably increases under pressure. The T_{md} denotes temperature at which the single-domain magnetic state converts to the multidomain one. Two possible spin configurations above and below T_{sw} are shown. The insets show an increase in the Néel temperature T_{N} and in the compensation temperature T_{comp} (top), as well as in the spin-reorientation temperature T_{SR} (bottom) under pressure.

temperature range 10–200 K and in magnetic field up to 10 kOe, using a PAR (model 4500) vibrating sample magnetometer. Magnetization measurements under hydrostatic pressure up to 10 kbar were performed using a miniature container of CuBe with an inside diameter of 1.4 mm [22] exploiting the silicon oil as a pressure-transmitting medium. Pressure at low temperatures was determined by the known pressure dependence of the superconducting transition temperature of pure tin. We used a cylindrical GdCrO_3 sample ≈ 2.4 mm long and ≈ 1.2 mm in diameter, cut from the original crystal in such a way that the c axis of the crystal, along which the FM moment is directed, lies in a plane perpendicular to the cylinder axis. Applied magnetic field H was directed perpendicularly to the cylinder axis. To obtain an accurate orientation of the c axis along the applied magnetic field, measurements of angular dependence of magnetization were performed each time when the sample was installed in the magnetometer, following applying hydrostatic pressure. Next temperature- and field-dependent magnetization of GdCrO_3 was measured along the FM easy axis.

III. RESULTS AND DISCUSSION

Figure 1 presents temperature dependencies of field-cooled (FC) magnetization of GdCrO_3 measured in magnetic field applied along the c axis upon cooling in 100 Oe at ambient pressure and at 10.1 kbar. The M vs T curves exhibit a series of changes, corresponding to successive magnetic transitions that occur at the following temperatures: (1) The Néel temperature $T_{\text{N}} = 168$ K at which the canted AFM order of Cr spins following a weak FM moment pointed along the c axis

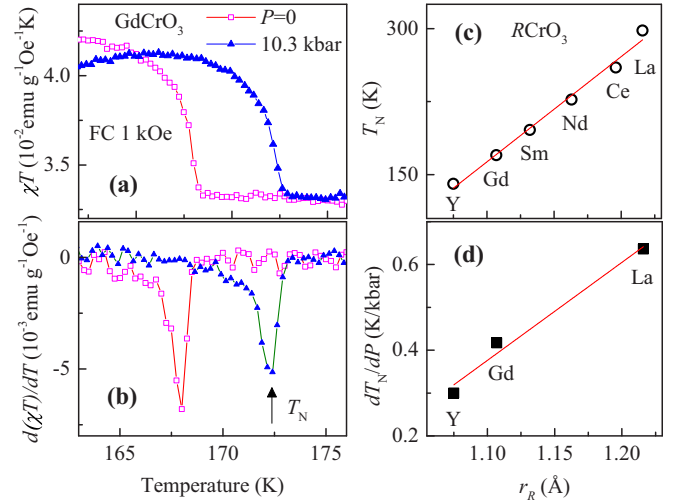


FIG. 2. (a) Temperature dependence of magnetic susceptibility multiplied by temperature χT . (b) Its derivative $d(\chi T)/dT$ derived from the FC magnetization of GdCrO_3 measured at $H = 1$ kOe applied along the c axis at $P = 0$ and 10.3 kbar. Peaks in $d(\chi T)/dT$ indicate the magnetic Cr^{3+} ordering temperatures. (c) The Néel temperature T_{N} and (d) pressure coefficient dT_{N}/dP of RCrO_3 orthochromites as function of the rare-earth ionic radius r_{R} (T_{N} of RCrO_3 and dT_{N}/dP for $R = \text{Y, La}$ are taken from Refs. [20,21,26,27]).

appears. (2) The compensation temperature T_{comp} at which two opposite magnetic moments, FM moment of canted Cr spins and paramagnetic moment of Gd spins induced by AFM coupling between Cr^{3+} and Gd^{3+} ions, cancel each other so that the net magnetization vanishes. (3) The spin switching temperature T_{sw} at which the magnetization reverses suddenly, changing its sign from the negative to the positive one. A metastable state with negative magnetization arises between the temperatures T_{comp} and T_{sw} when FM moment is directed against the applied magnetic field. (4) The temperature T_{md} below which the single-domain magnetic state converts to the multidomain one. (5) Finally, the spin-reorientation temperature $T_{\text{SR}} = 6.5$ K when the FM moment rotates from the c axis to the a axis. It appears that the applied pressure leads to an increase in all of the above characteristic temperatures, with the exception of the temperature T_{md} , which depends only on demagnetizing factor of the sample and applied magnetic field. Next, we will sequentially consider the possible nature of pressure effect on the magnetism of GdCrO_3 , taking into account appropriate interactions between magnetic ions. Of particular interest is an unexpectedly strong pressure-induced increase in the spin switching temperature T_{sw} .

For an accurate determination of the Néel temperature T_{N} under pressure, magnetic susceptibility multiplied by temperature χT (here χ was measured at $H = 1$ kOe applied along the c axis) and its derivative with respect to temperature, $d(\chi T)/dT$, were plotted versus temperature [see Figs. 2(a) and 2(b)]. According to the Fisher relation [23,24], temperature variation in quantity $d(\chi T)/dT$ is analogous to the changes in magnetic specific heat in canted antiferromagnet around T_{N} . Consequently, this manner provides a correct valuation of the ordering temperature of the Cr^{3+} moments

under pressure, shown by well resolved peaks in $d(\chi T)/dT$ in Fig. 2(b). Based on this approach, the pressure coefficient $dT_N/dP = +0.42$ K/kbar for GdCrO_3 is determined.

The nature of effect of physical and chemical pressure on T_N in $R\text{CrO}_3$ orthochromites is currently the subject of intensive studies [18,21,25,26]. Zhou and Goodenough have claimed that orthochromites with lower degree of CrO_6 octahedral-site rotation (tilts) exhibit a higher T_N [25]. It occurs because the superexchange interaction J , determining $T_N \sim J$ within the mean-field theory, is proportional to the square of the orbital overlap integral over the Cr–O–Cr bond, which is directly related to the Cr–O bond length l and the Cr–O–Cr tilt angle ϕ through the relationship $J \sim \cos^4[(180 - \phi)/2]/l^7$. In addition, the effect of hybridization of t and e orbitals due to the local site distortion [25,18] is important to explain the observed dramatic change in T_N across the $R\text{CrO}_3$ family shown in Fig. 2(c). Here, the T_N decreases and the octahedral-site rotations (structural distortions) increase with a change in the rare-earth ionic radius from La to Y, presenting a strong chemical pressure effect. The effect of external hydrostatic pressure on T_N also depends markedly on the size of R ions in $R\text{CrO}_3$ according to dT_N/dP data obtained for LaCrO_3 [26] and YCrO_3 [27], shown in Fig. 2(d). Zhou [18] explained this dependence by the fact that, under pressure, the octahedral-site rotations increase in $R\text{CrO}_3$ with a small R ion, but they become suppressed in compounds containing a large R ion. Namely, the increase in T_N under pressure is mainly due to shortening Cr–O bond length l , which weakly varies across the $R\text{CrO}_3$ series. However, in the case of small R ion size the effect appears to be compensated by pressure-induced bending of Cr–O–Cr bond angle away from 180° , resulting in a low coefficient dT_N/dP . The value of pressure coefficient obtained here for GdCrO_3 is in good agreement with this trend [see Fig. 2(d)].

The compensation temperature T_{comp} increases by about 3 K at applied pressure of 10.1 kbar, as shown in the upper inset in Fig. 1. This pressure-induced change in T_{comp} can be understood using a simple phenomenological model that successfully describes most of the specific FM behavior of GdCrO_3 [6,7], including spin switching around T_{comp} [8]. This approximation takes into account the canted FM moment of Cr spins, due to the DM interaction, and the opposite paramagnetic moment of Gd^{3+} induced by the AFM interaction between Cr^{3+} and Gd^{3+} spins, so the temperature dependence of magnetization at small applied field H is expressed as

$$M = M_{\text{Cr}} + C_{\text{Gd}}(-H_1 + H)/(T + \theta). \quad (1)$$

Here, M_{Cr} is the magnetization of canted Cr spins, C_{Gd} is the Curie constant, $C = Ng^2\mu_B^2S(S+1)/3k_B$, equal to 0.0306 emu K/g, according to calculation for the Gd^{3+} ground state with spin $S = 7/2$, H_1 is the internal exchange field associated with induced paramagnetic moment of Gd^{3+} spins, directed opposite the magnetization M_{Cr} , and $\theta = 2.3$ K [7] is the Weiss temperature, linked to the AFM interaction between Gd^{3+} spins. According to Eq. (1), the temperature T_{comp} at which magnetization in small field H vanishes is determined by the H_1 to M_{Cr} ratio: $T_{\text{comp}} = (C_{\text{Gd}}H_1/M_{\text{Cr}}) - \theta$. Some evidence of the likely changes in H_1 and M_{Cr} under pressure was obtained by fitting Eq. (1) with H_1 , M_{Cr} , and θ as varying parameters to the $M(T)$ curve measured in magnetic

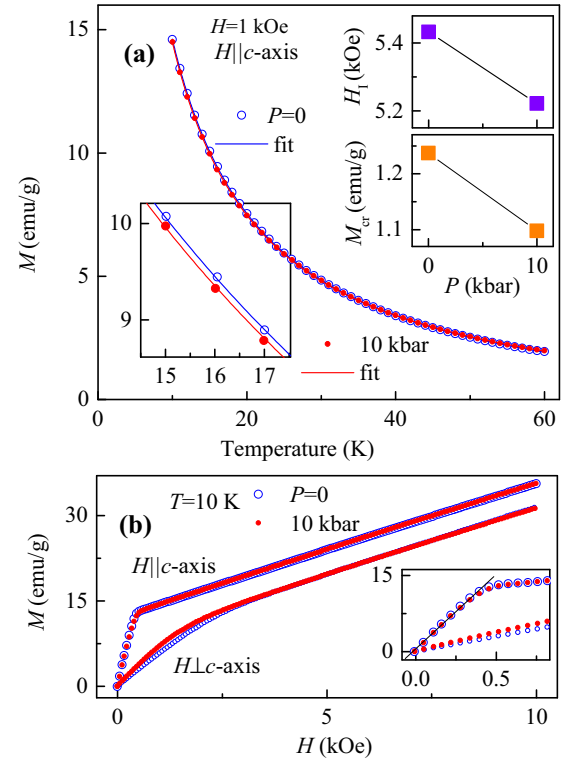


FIG. 3. (a) Temperature dependencies of magnetization measured between 10 and 60 K along the c axis at field of 1 kOe, at $P = 0$ and 10 kbar. Lines represent fit with Eq. (1) with fitting parameters H_1 , M_{Cr} , and θ . The upper insets show their change under pressure while the lower inset shows difference in the $M(T)$ curves and their fits at low T . (b) M vs H curves at 10 K measured at $P = 0$ and 10 kbar in magnetic field applied along the c axis and perpendicularly to the c axis.

field 1 kOe applied along the c axis at $P = 0$ and 10 kbar [see Fig. 3(a)]. The analyzed temperature range was well below T_N where the canted FM moment of Cr ions is mostly saturated. Note also that the magnetization measured in relatively large field, shown in Fig. 3(a), changes smoothly with decreasing temperature down to 10 K (there is a single magnetic domain state only) in contrast to that measured in the field of 100 Oe at which the transition to the multidomain state occurs below temperature $T_{\text{md}} \approx 35$ K (see Fig. 1). At 10 K, the multidomain magnetic state transforms into a single-domain state at field H equal to 390 Oe, at which the magnetization M reaches the value of 13 emu/g [see Fig. 3(b)] and the demagnetizing field $H_d = -4\pi N M d = -390$ Oe completely compensates for the applied field in the case of a multidomain state. Here, $d = 7.3$ g/cm³ is the density of GdCrO_3 and the demagnetizing factor $4\pi N = 4.1$. The very similar demagnetizing factor N can be estimated from the $M(T)$ data presented in Fig. 1. Namely, the value $M = 3.3$ emu/g ($Md = 24.1$ Oe), which remains constant below T_{md} at $H = 100$ Oe, means that the effective field inside the sample is zero, while the volume magnetic susceptibility $\chi_v = Md/H = 0.24$ reaches a value of $1/4\pi N$, which is a good proof of the multidomain state for the case of an easy-axis ferromagnet.

The results of fitting show that applied pressure causes a decrease in all H_1 , M_{Cr} , and θ values. Under pressure of

10 kbar, the effective field H_I decreases by about 4%, from 5433 ± 11 Oe at $P = 0$ to 5222 ± 17 Oe at 10 kbar, while the magnetization of canted Cr ions M_{Cr} is reduced by about 11%, from 1.237 ± 0.006 emu/g at $P = 0$ to 1.098 ± 0.009 emu/g at 10 kbar [see upper insets in Fig. 3(a)], and θ changes from 2.44 ± 0.02 K to 2.23 ± 0.03 K. Such changes in H_I , M_{Cr} , and θ should lead to an increase in the H_I/M_{Cr} ratio and, therefore, could explain the pressure-induced increase of the compensation temperature T_{comp} in accordance with Eq. (1). The $\Delta T_{comp}^{calc} = +11$ K, change in T_{comp} under applied pressure of 10 kbar, calculated with the above estimated changes in H_I , M_{Cr} , and θ , is in qualitative agreement with the observed increase in T_{comp} by 3 K. From the above analysis, it can be concluded that the suppression of the weak FM moment is the main reason for the increase in T_{comp} under pressure in GdCrO₃. The pressure-induced variation of canted FM moment arising from the DM interaction has not been experimentally investigated in orthochromites. Nevertheless, this effect has been studied theoretically for SmCrO₃ using the first-principles calculations, and a decrease in FM moment by about 20% was predicted with increasing external pressure to 100 kbar [20]. In addition, for the RCrO₃ series, a strong chemical pressure effect was calculated, suggesting a twofold increase in the weak FM moment when the rare-earth ion radius r_R decreases from 1.20 Å for $R = Ce$ to 1.06 Å for $R = Er$ [20]. Thus, the pressure-induced changes in the weak FM moment of GdCrO₃, estimated above, are in qualitative agreement with those predicted theoretically.

Let us discuss the possible effect of applied pressure on the nature of complex exchange interaction between Cr³⁺ and Gd³⁺ spins, which is the most important for exotic magnetism in GdCrO₃. The Cr–Gd exchange interaction includes isotropic exchange and noticeable symmetric and antisymmetric components of the anisotropic exchange, despite the fact that Gd³⁺ is an S ion [28,29]. The antisymmetric exchange was found to be responsible for the spin-reorientation transition $\Gamma_4 \rightarrow \Gamma_2$, which occurs at the temperature $T_{SR} = 6.5$ K [29]. It has been also calculated in Ref. [30], based on the magnetization data [7], that the contribution of antisymmetric exchange $\beta^{as} = 4.7$ kOe to the effective exchange field H_I dominates over the contribution of isotropic exchange $\alpha = 1.3$ kOe, while the contribution from anisotropic symmetric exchange is negative: $\beta^s = -0.5$ kOe, where $H_I = \alpha + \beta^{as} + \beta^s = 5.5$ kOe. According to the data shown in the lower inset of Fig. 1, the spin-reorientation temperature T_{SR} increases by about 1 K at an applied pressure of 10 kbar. It follows that the antisymmetric exchange β^{as} increases with pressure. However, the anisotropy energy associated with spin switching in GdCrO₃ noticeably decreases under pressure (we will show this below); therefore, the contribution of anisotropic exchange $|\beta^s|$ should also decrease. Thus, we can conclude that effective exchange field H_I decreases under pressure due to weakening of isotropic exchange α .

Figure 1 demonstrates that pressure effect on the spin switching temperature T_{sw} is the strongest among the others: T_{sw} increases by more than 20 K under pressure of 10 kbar. Knowledge of the reason for this behavior can help us in understanding the nature of spin switching. Figures 4(a) and 4(b) show also that the magnitude of the pressure effect is maximal at small applied cooling fields H , at which switching occurs

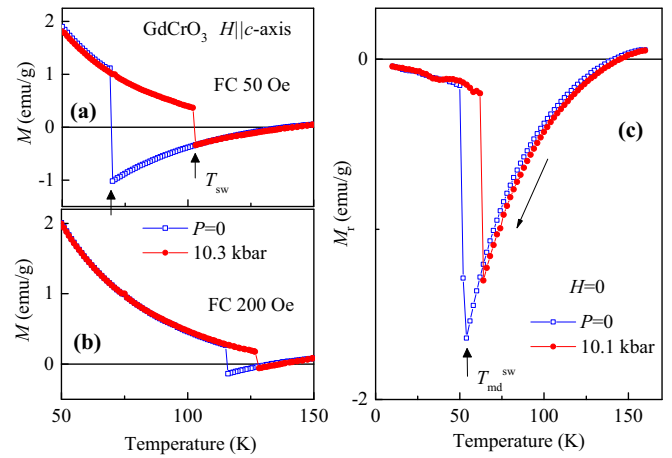


FIG. 4. Spin switching (spontaneous magnetization reversal along the c axis) in GdCrO₃ upon cooling in a field of 50 Oe (a) and 200 Oe (b), at $P = 0$ and 10.3 kbar. The switching temperature T_{sw} increases under pressure. (c) Remanent magnetization M_r measured along the c axis upon cooling at $H = 0$, after cooling at 1 kOe to a temperature of 160 K. Spin switching at temperature T_{md}^{sw} , after which M_r becomes close to zero, is associated with a transition to a multidomain state.

at low T_{sw} . Under this condition, the magnetization changes sign at T_{sw} , remaining practically unchanged in modulus [see Fig. 4(a)], since the paramagnetic contribution induced by a small field H is insignificant. The spontaneous spin switching is actually a first-order transition from a metastable state with negative magnetization (in this spin configuration the Zeeman energy $E_Z = -MH$ is maximal) to an equilibrium state with positive magnetization and minimal energy E_Z . Consequently, the system must spend the energy required for magnetization reversal by 180° along the c axis in order to overcome the anisotropy energy E_a . This energy should be equal to the drop in the Zeeman energy ΔE_Z at T_{sw} . Therefore, spin switching occurs at that temperature at which the modulus of negative magnetization becomes large enough for ΔE_Z to reach the energy barrier E_a . The ΔE_Z value can be evaluated directly from the data for $H = 50$ Oe shown in Fig. 4(a). As a result, we find that at ambient pressure ΔE_Z is nearby 100 erg/g, while at a pressure of 10 kbar it is much lower, about 35 erg/g. This means that the energy of magnetic anisotropy E_a decreases significantly under pressure. A similar conclusion also follows from an analysis of temperature dependence of remanent magnetization M_r vs T presented in Fig. 4(c). Here, M_r is the magnetization measured along the c axis upon cooling in zero magnetic field, at $P = 0$ and 10.1 kbar, for the sample cooled prior the measurements to 160 K in 1 kOe. However, in the absence of an applied field H , the reversal of the entire magnetization does not occur, but it takes place only in selected domains of the sample in order to reduce the magnetization and minimize the energy. Consequently, a sharp drop in M_r at T_{md}^{sw} indicates a transition from a single-domain state to a multidomain state with M_r close to zero (note that in the case of the negative magnetization state, this transition occurs via spin switching, in contrast to what occurs for the positive magnetization state shown in Fig. 1, at $T_{md} \approx 35$ K). Again, we see that temperature T_{md}^{sw} increases under pressure, whereas

the Zeeman energy drop ΔE_Z decreases from about 80 to near 50 erg/g. Here, ΔE_Z was calculated at $T_{\text{md}}^{\text{sw}}$ taking into account the fact that the real field inside the sample at $H = 0$ is the demagnetizing field $-4\pi N M d$, which in the single-domain state reaches the maximum values of 50 and 40 Oe at $P = 0$ and 10 kbar, respectively.

The change in the Zeeman energy ΔE_Z upon spin switching with a change in the magnetization from negative M to positive M is a measure of the energy barrier that the system must overcome in order to go from a metastable state to a thermodynamically equilibrium state with positive M . Obviously, the energy barrier in this case is the energy of magnetic anisotropy, that is, the energy required to deflect the magnetization of the crystal from an easy direction to a hard one. It is well explained in recent review of the phenomenon of negative magnetization by Kumar and Yusuf [31] that the presence of a finite magnetic anisotropy appears to be essential for an observation of the negative magnetization in compensating ferrimagnets. Namely, in the absence of a magnetic anisotropy, the compensated magnetics will show only a magnetic compensation behavior but without any negative magnetization and therefore spontaneous spin switching (magnetization reversal). This occurs because at zero anisotropy energy (no energy barrier), the net magnetization always corresponds to the direction of the applied field H , above and below T_{comp} .

The spin-switching anisotropy energy E_a contains two main contributions: one of GdCrO₃ intrinsic magnetocrystalline, E_a^{intr} , and the other of magnetic shape anisotropy (or dipolar anisotropy), E_a^{sh} , and thus, the spin switching parameters should depend on the sample shape. Indeed, we previously observed much lower switching temperatures T_{sw} when measuring a *long* GdCrO₃ sample of an elongated parallelepiped shape with a small demagnetizing factor of $4\pi N = 0.78$ along the c axis [8]. Moreover, the evaluated switching energy ΔE_Z turned out to be more than twice as high [8] as compared to that found in the sample under study. The different magnetic behavior can be simply explained by the presence of an additional energy barrier equal to difference in the demagnetizing energy $E_a^{\text{sh}} = 2\pi N M^2 d$ between the hard and easy magnetization directions, which must be overcome to rotate the magnetization vector by 180°. A rough estimation gives $E_a^{\text{sh}} \approx 100$ erg/g for the *long* sample with demagnetizing factors of 0.78 along the c axis and of about 6 for a direction perpendicular to the c axis, taking into account that in a field of 50 Oe the magnetization reaches -2.3 emu/g at T_{sw} (see Fig. 1 in Ref. [8]). On the contrary, for the sample under study, for which the factor $4\pi N = 4.1$ along the c axis is maximal in comparison with that for all other directions in the crystal, the E_a^{sh} energy contribution is absent. Consequently, it can be expected that the energy $\Delta E_Z = 100$ erg/g estimated above is close to the intrinsic anisotropy energy of GdCrO₃. Such a low energy in the present case of uniaxial anisotropy is consistent with a small value of the weak FM moment of Cr ions. In other words, a small switching energy is required to reverse the moment of Cr ions by rotating the AFM-ordered canted spins Cr by a small angle 2γ , where $\gamma \sim 0.5^\circ$ is the canting angle in GdCrO₃. Note that in the sample under study, which is characterized only by intrinsic anisotropy, the switching temperature T_{sw} is maximal for a

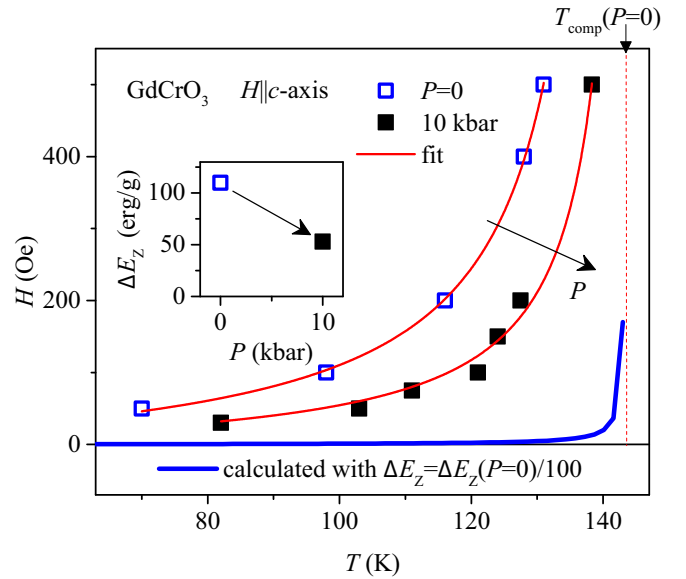


FIG. 5. $T_{\text{sw}}-H_{\text{sw}}$ boundary between magnetic phases with opposite spin configurations at $P = 0$ and 10 kbar. The lines represent the best fit with Eq. (2) for two parameters, $\Delta E_Z/2M_{\text{Cr}}$ and T_{comp} . The bold line is calculated using Eq. (2) with the same M_{Cr} and T_{comp} as for $P = 0$, but with the value of ΔE_Z two orders of magnitude lower than the value at $P = 0$. The inset shows the decrease in the spin switching energy ΔE_Z under pressure.

given applied field H . However, a much smaller value of T_{sw} is observed for the same field H in the sample, which additionally has the strong magnetic shape anisotropy. Thus, the spin switching temperature in compensated GdCrO₃ ferrimagnet can be controlled by the change of the sample shape.

Figure 5 shows the switching temperatures T_{sw} at various applied field H , derived from M vs T curves similar to those shown in Figs. 4(a) and 4(b), at $P = 0$ and 10 kbar. It is clearly seen that the line $T_{\text{sw}}-H_{\text{sw}}$, which is the boundary between magnetic phases with two opposite spin configurations, as shown in Fig. 1, noticeably shifts towards higher temperatures under pressure. It was previously reported [8] that this boundary between the metastable state with negative magnetization and the equilibrium magnetic state can be qualitatively described in GdCrO₃ by the phenomenological model predicting Eq. (1). According to Eq. (1), the fall in the Zeeman energy at spin switching is equal to $\Delta E_Z = -2(M_{\text{Cr}} - C_{\text{Gd}}H_1/T)H_{\text{sw}}$ and, taking into account that $T_{\text{comp}} = (C_{\text{Gd}}H_1/M_{\text{Cr}}) - \theta$, the switching field H_{sw} as a function of temperature can be expressed for temperatures $T < T_{\text{comp}}$ as follows:

$$H_{\text{sw}} = -(\Delta E_Z/2M_{\text{Cr}})(T + \theta)/(T - T_{\text{comp}}). \quad (2)$$

The H_{sw} vs T dependence was compared with experimental data under the assumption that the $\Delta E_Z/M_{\text{Cr}}$ ratio does not change with temperature (note that in this approximation, both ΔE_Z and M_{Cr} should change with temperature in accordance with the Brillouin function with spin $S_{\text{Cr}} = 3/2$ [29,32]). The solid lines in Fig. 5 are the best fit with Eq. (2) for the values of fitting parameters $\Delta E_Z/2M_{\text{Cr}} = 46.8 \pm 1.4$ Oe and $T_{\text{comp}} = 143.4 \pm 0.5$ K and $\Delta E_Z/2M_{\text{Cr}} = 24 \pm 2$ Oe and $T_{\text{comp}} = 145 \pm 0.7$ K obtained for $P = 0$ and 10 kbar,

respectively. Taking into account that the saturated canted FM moment of Cr ions decreases from 1.237 to 1.098 emu/g under pressure of 10 kbar, as determined above, we estimate the switching energies ΔE_Z to be equal to 116 and 53 erg/g at $P = 0$ and 10 kbar, respectively. It appears that ΔE_Z decreases by half at a pressure of 10 kbar (see inset to Fig. 5). Remarkably, the ΔE_Z values obtained by fitting Eq. (2) to the $T_{sw}-H_{sw}$ phase boundary are close to those calculated above directly from the magnetization jump at spin switching, shown in Fig. 4(a). In addition, the above fit results predict also an increase in the compensation temperature T_{comp} under pressure in accordance with the observed shift $\Delta T_{comp}^{exp} = +3$ K. Thus, a strong shift of the $T_{sw}-H_{sw}$ line towards higher temperatures under pressure (see Fig. 5) is caused, first of all, by a significant decrease in the magnetic anisotropy and, by the second factor, the rise of compensation temperature T_{comp} . Recall that the increase in T_{comp} under pressure in GdCrO₃ is mainly determined by the suppression of the weak FM moment of Cr ions. The model used, where the ΔE_Z in Eq. (2) has the meaning of the energy of magnetic anisotropy, well describes the transformation between magnetic phases with opposite spin configurations in GdCrO₃ due to a decrease in the anisotropy. This predicts that the phase with negative magnetization as well the spontaneous spin switching will almost disappear (or in other words, the magnetization becomes positive already in a very small field H) if the ΔE_Z (energy barrier) is two orders of magnitude lower than that estimated at $P = 0$; see the calculated line in Fig. 5.

Additional evidence of the weakening of the magnetic anisotropy under pressure in GdCrO₃ can be obtained from the angular dependence of the magnetization $M(\varphi)$ measured for selected temperatures $T < T_{comp}$ at $P = 0$ and 10.2 kbar, presented in Fig. 6. Here, the magnetization was measured along the applied magnetic field $H = 100$ Oe, which rotates 360° in the plane containing the c axis, and φ is the angle between the vector \mathbf{H} and the c axis. With decreasing temperature, the $M(\varphi)$ curves demonstrate an exceptional evolution from a hard magnetic behavior to the soft one. Namely, the magnetization vector at $T = 110$ K remains in its original position despite the fact that the field H changes its direction to the opposite one, providing the state with negative magnetization [see Fig. 6(a)]. It is due to the high anisotropy of canted FM moment of Cr ions, which dominates over the soft paramagnetic moment of Gd spins; therefore, the applied field of 100 Oe is too small, compared to the field $H_{sw} = 160$ Oe, required for switching at $T = 110$ K (see the $T_{sw}-H_{sw}$ line for $P = 0$ in Fig. 5). In this case, the $M(\varphi)$ dependence is described by a simple $\cos\varphi$ dependence; see the fitted line in Fig. 6(a). On contrary, the increased soft Gd-spin moment at $T = 50$ K is dominant in the system, therefore the field of 100 Oe is large enough to provide the equilibrium state at this temperature (see Fig. 5). In this case, the magnetization changes sign coherently with the vector H and exactly follows the typical dependence $M \sim |\cos\varphi|$ for ferromagnets with uniaxial anisotropy [33]; see fitted line in Fig. 6(c). At 90 K, two contributions to magnetic anisotropy from the hard Cr spins and the soft Gd spins compete and lead to the appearance of a metastable state with negative magnetization at the angles $\varphi > 90^\circ$. Further, the switching to the equilibrium state occurs at an angle $\varphi \approx 130^\circ$, when the projection of \mathbf{H} onto the c axis

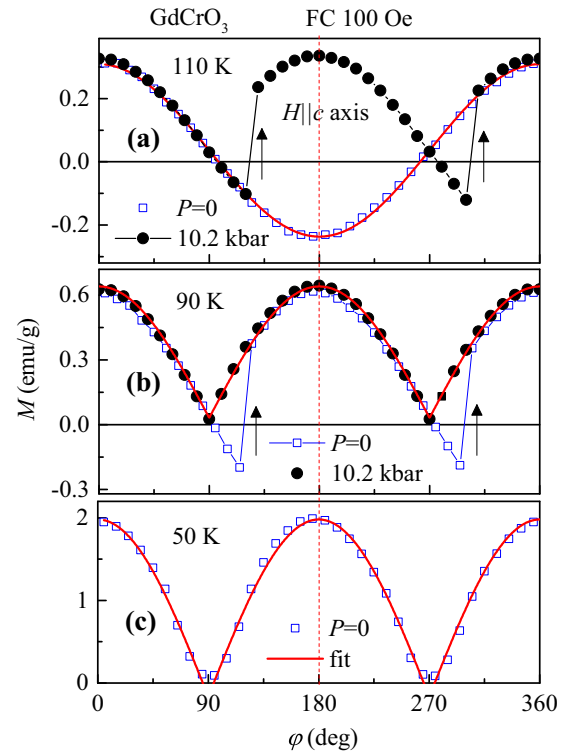


FIG. 6. The angular dependence of magnetization $M(\varphi)$ of GdCrO₃ ferrimagnet measured for temperatures $T < T_{comp}$ at $P = 0$ and 10.2 kbar along the applied magnetic field $H = 100$ Oe, which rotates 360° in the plane containing the c axis (here φ is the angle between the vector \mathbf{H} and the c axis). Applied pressure induces the spin switching (magnetization changes sign from negative to positive) at 110 K (a), while it suppresses the switching at 90 K (b). The solid lines are the best fits using the $M \sim \cos\varphi$ (a) and $M \sim |\cos\varphi|$ (b), (c) dependencies.

reaches the critical value of H_{sw} . This behavior is analogous to the spin switching caused by a decrease in temperature shown in Figs. 1 and 4, and the critical value $H_{sw} \approx 70$ Oe, calculated for $T = 90$ K as $H\cos(180^\circ - \varphi) - 4\pi N M d$, is in excellent agreement with the H_{sw} value corresponding to the line $T_{sw}-H_{sw}$ for $P = 0$ in Fig. 5.

Applied pressure of 10 kbar radically changes the $M(\varphi)$ dependence at 110 K [see Fig. 6(a)]. Namely, the magnetization switches from negative to positive, in the same way as it happens at $P = 0$ at 90 K, when the projection of \mathbf{H} on the c axis exceeds the value of $H_{sw} \approx 75$ Oe required to switch spins at $P = 10$ kbar; see line $T_{sw}-H_{sw}$ in Fig. 5. On the contrary, at $T = 90$ K, the pressure blocks spin switching and transforms the $M(\varphi)$ dependence into $M \sim |\cos\varphi|$ one; see Fig. 6(b). Both specific behaviors, as well as the fact that the switching fields H_{sw} , obtained from different curves $M(T)$ and $M(\varphi)$, coincide, convincingly prove that the spin switching energy, and hence the anisotropy energy of GdCrO₃, decreases under pressure. It is interesting to note that the external pressure acts similarly to the applied magnetic field along the c axis, moving the switching temperature T_{sw} towards the compensation temperature T_{comp} , as shown in Figs. 4(a) and 4(b). It is clear that both pressure and magnetic field suppress the uniaxial

anisotropy; therefore, one should expect the disappearance of spin switching as a whole at sufficiently large values of P and H . Recall that in GdCrO_3 with a low intrinsic anisotropy, the temperature T_{sw} can be noticeably reduced by increasing magnetic anisotropy due to the change of the sample shape. This behavior illuminates the nature of the spin switching in GdCrO_3 .

IV. CONCLUSIONS

It was found that in GdCrO_3 single crystal both the Néel and the compensation temperatures increase under pressure, which can be explained by an increase in the exchange interaction between Cr spins, a decrease in the weak FM moment

caused by canted Cr spins, and a weakening of the interaction between the Cr and Gd spins. The observed strong increase in the spin switching temperature T_{sw} under pressure is attributed to a decrease in magnetic anisotropy. Namely, the spin switching energy associated with uniaxial anisotropy decreases by half at a pressure of 10 kbar, which shifts the spin switching line in the T - H diagram towards higher temperatures. According to this mechanism, switching between two opposite spin configurations can be controlled by external pressure. On the other hand, due to the low intrinsic anisotropy of GdCrO_3 , the temperature T_{sw} can be also varied by changing the magnetic anisotropy caused by the change of the sample shape. The revealed features clarify the nature of spontaneous spin switching in the compensated GdCrO_3 ferrimagnet.

-
- [1] B. Rajeswaran, D. I. Khomskii, A. K. Zvezdin, C. N. R. Rao, and A. Sundaresan, *Phys. Rev. B* **86**, 214409 (2012).
- [2] L. H. Yin, J. Yang, X. C. Kan, W. H. Song, J. M. Dai, and Y. P. Sun, *J. Appl. Phys.* **117**, 133901 (2015).
- [3] Y. Zhu, P. Zhou, T. Li, J. Xia, S. Wu, Y. Fu, K. Sun, Q. Zhao, Z. Li, Z. Tang, Y. Xiao, Z. Chen, and H.-F. Li, *Phys. Rev. B* **102**, 144425 (2020).
- [4] S. Mahana, B. Rakshit, R. Basu, S. Dhara, B. Joseph, U. Manju, S. D. Mahanti, and D. Topwal, *Phys. Rev. B* **96**, 104106 (2017).
- [5] S. Mahana, U. Manju, P. Nandi, E. Welter, K. R. Priolkar, and D. Topwal, *Phys. Rev. B* **97**, 224107 (2018).
- [6] K. Yoshii, *J. Solid State Chem.* **159**, 204 (2001).
- [7] A. H. Cooke, D. M. Martin, and M. R. Wells, *J. Phys. C: Solid State Phys.* **7**, 3133 (1974).
- [8] I. Fita, R. Puzniak, A. Wisniewski, and V. Markovich, *Phys. Rev. B* **100**, 144426 (2019).
- [9] M. Tripathi, T. Chatterji, H. E. Fischer, R. Raghunathan, S. Majumder, R. J. Choudhary, and D. M. Phase, *Phys. Rev. B* **99**, 014422 (2019).
- [10] J.-H. Lee, Y. K. Jeong, J. H. Park, M.-A. Oak, H. M. Jang, J. Y. Son, and J. F. Scott, *Phys. Rev. Lett.* **107**, 117201 (2011).
- [11] J.-S. Jung, A. Iyama, H. Nakamura, M. Mizumaki, N. Kawamura, Y. Wakabayashi, and T. Kimura, *Phys. Rev. B* **82**, 212403 (2010).
- [12] S. Yuan, W. Ren, F. Hong, Y. B. Wang, J. C. Zhang, L. Bellaïche, S. X. Cao, and G. Cao, *Phys. Rev. B* **87**, 184405 (2013).
- [13] S. Cao, H. Zhao, B. Kang, J. Zhang, and W. Ren, *Sci. Rep.* **4**, 5960 (2014).
- [14] Y. Sun, J.-Z. Cong, Y.-S. Chai, L.-Q. Yan, Y.-L. Zhao, S.-G. Wang, W. Ning, and Y.-H. Zhang, *Appl. Phys. Lett.* **102**, 172406 (2013).
- [15] Y. Cao, S. Cao, W. Ren, Z. Feng, S. Yuan, B. Kang, B. Lu, and J. Zhang, *Appl. Phys. Lett.* **104**, 232405 (2014).
- [16] I. Fita, A. Wisniewski, R. Puzniak, V. Markovich, and G. Gorodetsky, *Phys. Rev. B* **93**, 184432 (2016).
- [17] I. Fita, A. Wisniewski, R. Puzniak, E. E. Zubov, V. Markovich, and G. Gorodetsky, *Phys. Rev. B* **98**, 094421 (2018).
- [18] J.-S. Zhou, *Phys. Rev. B* **101**, 224104 (2020).
- [19] V. S. Bhadram, D. Swain, R. Dhanya, M. Polentarutti, A. Sundaresan, and C. Narayana, *Mater. Res. Express* **1**, 026111 (2014).
- [20] H. J. Zhao, W. Ren, X. M. Chen, and L. Bellaïche, *J. Phys.: Condens. Matter.* **25**, 385604 (2013).
- [21] J. S. Zhou, J. A. Alonso, V. Pomjakushin, J. B. Goodenough, Y. Ren, J. Q. Yan, and J. G. Cheng, *Phys. Rev. B* **81**, 214115 (2010).
- [22] M. Baran, V. Dyakonov, L. Gladczuk, G. Levchenko, S. Piechota, and H. Szymczak, *Physica C (Amsterdam, Neth.)* **241**, 383 (1995).
- [23] M. E. Fisher, *Philos. Mag.* **7**, 1731 (1962).
- [24] E. E. Bragg and M. S. Seehra, *Phys. Rev. B* **7**, 4197 (1973).
- [25] J. S. Zhou and J. B. Goodenough, *Phys. Rev. B* **77**, 132104 (2008).
- [26] J. S. Zhou, J. A. Alonso, A. Muoz, M. T. Fernandez-Diaz, and J. B. Goodenough, *Phys. Rev. Lett.* **106**, 057201 (2011).
- [27] J. S. Zhou and J. B. Goodenough, *Phys. Rev. Lett.* **89**, 087201 (2002).
- [28] T. Yamaguchi, *J. Phys. Chem. Solids.* **35**, 479 (1974).
- [29] S. Washimiya and C. Satoko, *J. Phys. Soc. Jpn.* **45**, 1204 (1978).
- [30] A. M. Kadomtseva, A. P. Agafonov, I. A. Zorin, A. S. Moskvin, T. L. Ovchinnikova, and V. A. Timofeeva, *Zh. Eksp. Teor. Fiz.* **84**, 1432 (1983) [*Sov. Phys. JETP* **57**, 833 (1983)].
- [31] A. Kumar and S. M. Yusuf, *Phys. Rep.* **556**, 1 (2015).
- [32] D. V. Belov, N. P. Kolmakova, I. B. Krynetskii, V. N. Milov, A. A. Mukhin, and V. A. Semenov, *Zh. Eksp. Teor. Fiz.* **88**, 1063 (1985) [*Sov. Phys. JETP* **61**, 624 (1985)].
- [33] F. Y. Yang, C. L. Chien, E. F. Ferrari, X. W. Li, Gang Xiao, and A. Gupta, *Appl. Phys. Lett.* **77**, 286 (2000).